

## NUMERICAL INVESTIGATION ON INITIAL POST-BUCKLING BEHAVIOUR OF COMPOSITE THIN-WALLED STRUCTURE

Jiayi. Yan<sup>1</sup>, Shuguang. Li<sup>2</sup>, Shihui Duan<sup>3</sup>

Institute of Aerospace Technology, Faculty of Engineering,  
University Of Nottingham, Nottingham, NG7 2RD, UK

<sup>1</sup> Email: emxjy3@nottingham.ac.uk

<sup>2</sup> Email: shuguang.li@nottingham.ac.uk,

Web Page: <https://www.nottingham.ac.uk/engineering/people/shuguang.li>

<sup>3</sup> Aircraft Strength Research Institute,  
Xi'an City, 710065, P.R.China

Email: duansh63@163.com

**Keywords:** initial post-buckling, curved shell, FE implementation, composite

### Abstract

The implementation of Koiter's initial post-buckling theory into FE is satisfactorily conducted with newly-established FE formulation. The analytical expression of first initial post-buckling coefficient for a simply supported composite curved shell has been employed for the validation of the numerical results. To reproduce conditions as employed in the analytical solution, i.e. the uniform displacement distribution in the pre-buckling regime, the boundary conditions are intentionally altered to obtain the desirable pre-buckling deformation. Five numerical simulations are carried out and both the buckling loads and the initial post-buckling coefficients show excellent agreement with analytical values. Realistic boundary conditions have been considered to predict the mechanical behaviours after bifurcation. The accuracy and reliability of this implementation of initial post-buckling theory in the context of finite elements have been achieved. The analysis is expected to be extended to more practical engineering problems.

### 1. Introduction

Curved panels are typical components in aero-structures, such as the skins of wings and fuselage. Meanwhile, to meet the high requirement of weight-strength ratio, composite material has drawn the attention and demonstrated its advantage in last decades as an alternative to metallic materials. For the upper airfoil, the compression loading condition is mainly encountered and frequently leads to the stability problem of structure. With the asymptotic expression of initial post-buckling displacement, Koiter's theory [1] conveys further information besides buckling load and buckling mode which are provided by conventional methods.

After the appearance of initial post-buckling theory, many researchers attempted to extend its application from its analytical presentation to finite element formulation. Most recently, Rahman and Jansen [2, 3] investigated structural stability with single-mode and multiple-mode into consideration. Lanzo [4] also made immense contribution to this area of research, including endeavour of using particular beam element and shell element, the structural imperfection sensitivity with regard to residual stress. Plenty of efforts were taken to reduce the computational time when generating the post-buckling curvature coefficient [4-11]. Principle of virtual work which was firstly proposed by Budiansky and Hutchinson [12] is utilised as the most popular strategy to implement Koiter's theory into computer program. The present work is based on the principle of stationary potential energy identical to the procedure in Koiter's thesis. To the best of knowledge of authors, although many

researchers have claimed their success of implementing initial post-buckling theory into finite element application, numerical results were not compared to analytical values.

The derivations of initial post-buckling slope, i.e. coefficient  $a$ , of orthotropic curved shell subjected to longitudinal compression with analytical method are presented. Five FE models with identical uniform pre-buckling deformation to analytical situations by using idealised boundary conditions are established. The numerical results are compared with the analytical ones and in order to demonstrate the influence of boundary conditions, consistent boundary conditions are imposed both in pre-buckling analysis and buckling calculation to compare the numerical outcomes.

## 2. Analytical expressions

The initial post-buckling coefficients contain insightful information of structural behaviours after the bifurcation point and after. For instance, if the post-buckling slope is not equal to zero or the post-buckling curvature is negative, an unstable post-buckling behaviour is expected and the conclusion of structure sensitivity to initial geometrical imperfection could be drawn as well. To curved shell, a non-vanished post-buckling slope often exists under some specific circumstances. The analytical expression of this coefficient is presented. The material is assumed to be orthotropic.

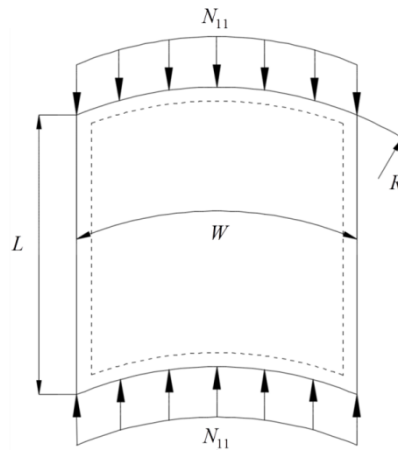


**Figure 1.** Curved shell under longitudinal compression

The governing equations of curved shell with simply supported boundary condition, as depicted in Figure 1, are following,

$$\begin{cases} L_{\phi\phi}\phi + \frac{1}{2}S(\omega, \omega) - \frac{1}{R}\omega_{,xx} = 0 \\ L_{\omega\omega}\omega - S(\omega, \phi) + \frac{1}{R}\phi_{,xx} = 0 \end{cases} \quad (1)$$

Where  $\omega$  is function of deflection,  $\phi$  the Airy stress function and  $R$  the radius of curved shell. The rest notations are defined as

$$S(\omega, \phi) = \omega_{,xx}\phi_{,yy} - 2\omega_{,xy}\phi_{,xy} + \omega_{,yy}\phi_{,xx} \quad (2)$$

$$L_{\phi\phi} = a_{22}(\ )_{,xxxx} + (2a_{12} + a_{66})(\ )_{,xxyy} + a_{11}(\ )_{,yyyy} \quad (3)$$

$$L_{\omega\omega} = D_{11}(\ )_{,xxxx} + 2(D_{12} + 2D_{66})(\ )_{,xxyy} + D_{22}(\ )_{,yyyy} \quad (4)$$

$[a]$  is the inverse of extensional stiffness matrix and  $[D]$  the bending stiffness matrix from classic lamination theory. Load  $\lambda$ , Airy stress  $\phi$  and deflection distribution  $\omega$  could be asymptotically expressed from the bifurcation point,

$$\lambda = \lambda^c (1 + a\xi + \dots) \quad (5)$$

$$\phi = \lambda \phi^{(0)} + \xi \phi^{(1)} + \xi^2 \phi^{(2)} + \dots \quad (6)$$

$$\omega = \lambda \omega^{(0)} + \xi \omega^{(1)} + \xi^2 \omega^{(2)} + \dots \quad (7)$$

$\lambda^c$  is the buckling load and  $\xi$  signifies the magnitude of perturbation. The substitutions of equations (5), (6) and (7) into equation (1) lead to a series of perturbation equations, the first perturbation equations are written as

$$\begin{cases} L_{\phi\phi} \phi^{(1)} - \frac{1}{R} \omega_{,xx}^{(1)} = 0 \\ L_{\omega\omega} \omega^{(1)} + \lambda^c \omega_{,xx}^{(1)} + \frac{1}{R} \phi_{,xx}^{(1)} = 0 \end{cases} \quad (8)$$

Without loss of generality, buckling mode could be assumed as

$$\omega = t \sin k\beta x \sin \beta y, \quad (9)$$

Where,  $t$  is assigned to the whole thickness of laminate,  $\beta = \pi/W$  and  $k = mW/L$ .  $m$  is the number of half wave along the longitudinal direction. The number of half wave along the circumferential direction is set to be one. By inserting equation (9) into equation (8), one can obtain the expression of  $\phi^{(1)}$  and buckling load,

$$\phi^{(1)} = -\frac{k^2 t}{R\beta^2 (a_{22}k^4 + (2a_{12} + a_{66})k^2 + a_{11})} \sin k\beta x \sin \beta y \quad (10)$$

$$\lambda^c = \frac{\beta^2 (d_{11}k^4 + 2(d_{12} + 2d_{66})k^2 + d_{22})}{k^2} + \frac{k^2}{R^2 \beta^2 (a_{22}k^4 + (2a_{12} + a_{66})k^2 + a_{11})} \quad (11)$$

In light of loading condition as shown in Figure 1, one unit uniform pressure is prescribed at the two ends so that

$$\begin{cases} \phi_{,yy}^{(0)} = -1 \\ \phi_{,xx}^{(0)} = \phi_{,xy}^{(0)} = 0 \end{cases} \quad (12)$$

According to [13], the post-buckling slope is function of buckling load, buckling mode and Airy stress,

$$a = -\frac{3}{2\lambda^c} \frac{\iint_A \left( \overset{(1)}{\phi}_{,yy} \overset{(1)}{\omega}_{,x} \overset{(1)}{\omega}_{,x} - 2 \overset{(1)}{\phi}_{,xy} \overset{(1)}{\omega}_{,x} \overset{(1)}{\omega}_{,y} + \overset{(1)}{\phi}_{,xx} \overset{(1)}{\omega}_{,y} \overset{(1)}{\omega}_{,y} \right) dA}{\iint_A \left( \overset{(0)}{\phi}_{,yy} \overset{(1)}{\omega}_{,x} \overset{(1)}{\omega}_{,x} - 2 \overset{(0)}{\phi}_{,xy} \overset{(1)}{\omega}_{,x} \overset{(1)}{\omega}_{,y} + \overset{(0)}{\phi}_{,xx} \overset{(1)}{\omega}_{,y} \overset{(1)}{\omega}_{,y} \right) dA} \quad (13)$$

Through the substitution of equations (10), (11) and (12) into equation (13), post-buckling coefficient  $a$  is updated as

$$a = \frac{8}{\lambda^c} \frac{1 - (-1)^m}{m\pi^2} \frac{k^2 t}{R(a_{22}k^4 + (2a_{12} + a_{66})k^2 + a_{11})} \quad (14)$$

It is easy to notice that the odd number of half wave in the longitudinal direction determines  $a$  as a positive value. With regard to the arbitrary distribution of initial geometrical imperfection, the structure is of unstable initial post-buckling behaviour after bifurcation. While the even number one makes  $a$  vanish. To discover the stability condition, second perturbation equations are supposed to be derived so as to generate the second initial post-buckling coefficient  $b$ .

### 3. Numerical results

Different kinds of boundary conditions have been taken into consideration. One is to duplicate the exact situation of pre-buckling regime of analytical expressions in section 2. Moreover, attention to boundary conditions of buckling calculation in accordance with analytical solutions is paid. The other one is to forcefully exert simply supported boundary conditions to the structure as reality and naturally the boundary conditions are extended to buckling analysis without any alteration.

#### 3.1. Idealised boundary conditions corresponding to the analytical solutions

To produce uniform pre-buckling deformation, there should be no constraints along both circumferential and radial direction so that no rotational displacement would occur. A cylindrical coordinate system is used to locate structure as shown in Figure 2. Z direction is parallel to the axis of shallow shell and RT plane parallel to both top and bottom ends. Point A and B are the vertexes of top and bottom curves. A 5-DOF (degree of freedom) reduced integration shell element is created in the coding. The 5 DOFs comprise of 3 translational DOFs and 2 rotational DOFs. The uniform displacement distribution is generated under the condition of two rotational DOFs of all nodes fixed. Additionally, translational DOFs along angular coordinate of point A and B are constrained as well along with the one along longitudinal direction of point B. One unit edge pressure is applied longitudinally on both top and bottom boundaries. The boundary conditions for calculation of buckling load are depicted in Figure 3. Translational DOFs along radial direction of four edges  $S_1$ - $S_4$  are fixed. Meanwhile, angular displacement of  $S_1$  and  $S_3$  and longitudinal deformation of  $S_2$  and  $S_4$  are restrained as well. The rotational DOFs of all nodes are set free in this analysis.

**Table 1.** Material properties

$E_{11}$ (GPa)	$E_{22}$ (GPa)	$G_{12} = G_{13}$ (GPa)	$G_{23}$ (GPa)	$\nu_{12}$
138	11.0	5.50	3.93	0.278

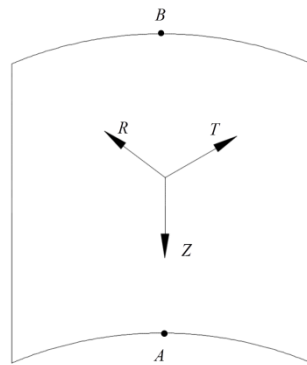


**Figure 2.** Boundary condition for uniform pre-buckling stress

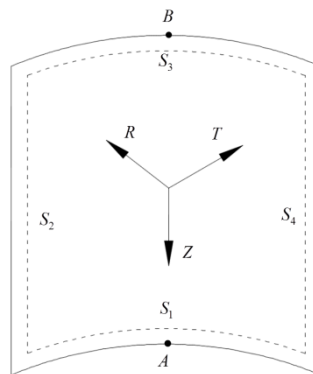


**Figure 3.** Simply supported boundary condition

The stacking sequence is  $[90/0/90/0]_s$ . Thickness of each layer is 0.125mm. The buckling mode is normalized by setting the maximum deflection equal to the total thickness of curved shell, viz.  $t$  in equation (9) equal to 1mm. Material properties are tabulated in Table 1. Five cases are calculated with analytical method and numerical approach, respectively. The results including buckling load and initial post-buckling slope are listed in Table 2.

**Table 2.** Comparisons of buckling loads and initial post-buckling slopes

$R(mm)$	$W(mm)$	$L(mm)$	$m$	Buckling load ( $N/mm$ )		$a$	
				AS*	NS-I*	AS	NS-I
200	34.9	20	1	159.46	154.62	0.2251	0.2314
200	34.9	50	2	134.81	131.71	0.0000	0.1012E-11
200	34.9	80	3	131.56	128.73	0.0971	0.1009
200	34.9	110	4	130.57	127.85	0.0000	0.1275E-9
200	34.9	140	5	130.16	127.52	0.0593	0.0704

\*AS: Analytical solution, NS-I: Numerical solution with idealised boundary conditions

With the variations of length of curved shell, one can observe different numbers of half wave in the longitudinal direction to generate sufficient and distinctive findings for comparison. It is easy to find out that the buckling loads calculated through self-coding program are satisfactorily consistent with analytical ones. In addition, the values of initial post-buckling slopes demonstrate the accuracy in contrast. Especially, for the cases with even numbers of half wave, negligibly infinitesimal values of  $a$  excellently predict the symmetric distribution of initial post-buckling behaviours of curved structure.

### 3.2. Consistent boundary conditions for pre-buckling and buckling analyses

To demonstrate the influence of boundary conditions on the buckling load and the initial post-buckling regime, simply supported boundary conditions as shown in Figure 2 are used both in pre-buckling analysis and calculation of buckling so that the uniform displacement distribution is no more guaranteed and buckling load is consequently slightly changed to some extent. It is worth noting that to produce a uniform pre-buckling deformation as much as possible, the angular and longitudinal displacement of four edges is set free different from the ones in buckling analysis of previous subsection. Nevertheless, the Point A and B are used to locate the global position of structure. The constraints of radial direction of four edges are performed. For the efficient comparisons of numerical results, same models are created in extensively-used commercial finite element software Abaqus. The structural dimensions are identical to the ones in Table 2. The values resulting from three approaches are listed in Table 3.

**Table 3.** Numerical values generated from different boundary condition

$m$	Buckling load ( $N/mm$ )			$a$	
	AS	Abaqus	NS-C*	AS	NS-C
1	159.46	146.56	147.23	0.2251	0.1346
2	134.81	125.31	126.27	0.0000	0.4327E12
3	131.56	123.02	123.93	0.0971	0.0526
4	130.57	122.39	123.28	0.0000	0.5280E-8
5	130.16	122.17	123.06	0.0593	0.0387

\* NS-C: Numerical solution with consistent boundary conditions

Although the numbers of half waves in longitudinal direction remain the same, the buckling loads either from Abaqus or self-programing package are consistently lower than analytical values. The excellent correlations of buckling loads between Abaqus and NS-C signify the accuracy of this program. In cases 2 and 4, the initial post-buckling slopes still tend to zero however a considerable reduction of  $a$  in cases 1, 3 and 5 can be readily observed. Consequently, one can perceive that the drastic differences in term of buckling load and  $a$  stem from the discrepancy of boundary conditions.

### 4. Conclusions

The Koiter's initial post-buckling theory is framed into finite element environment to generate the buckling load and first initial post-buckling coefficient of curved shell subjected to uniaxial compression. To compare to the analytical results, the material is specified to be orthotropic. The principle of stationary potential energy is adopted for the finite element formulation which is not presented in this paper due to the limitation of space.

Five configurations of curved shell with varying lengths are taken into consideration. Particular attention is paid to boundary conditions of pre-buckling and buckling analyses to reproduce the analytical values. Encouragingly satisfactory agreements between analytical and numerical results have been achieved. Significance of boundary conditions is demonstrated through the big discrepancy of buckling load and first initial post-buckling coefficient. The achievement of initial post-buckling curvature, i.e. coefficient  $b$ , is expected to be completed in the future work.

### Acknowledgments

The work is financially supported by the Aircraft Strength Research Institute of P.R.China.

## References

- [1] W.T. Koiter. On the Stability of Elastic Equilibrium. *Ph.D Thesis, Delft*, 1945.
- [2] T. Rahman, E.L. Jansen. Finite element based initial post-buckling analysis of shells of revolution. *49th AIAA/ASME/ASCE/AHS/ASC Structures, Structural Dynamics, and Materials Conference*, Illinois, United States, April 7-10 2008.
- [3] T.Rahman, E.L. Jansen. Finite element based coupled mode initial post-buckling analysis of a composite cylindrical shell. *Thin-Walled Structures*, 48: 25–32, 2010.
- [4] A.D. Lanzo, G. Garcea. Koiter's analysis of thin-walled structures by a finite element approach. *International Journal for Numerical Methods in Engineering*, 39: 3007–3031, 1996.
- [5] G. Salerno, A.D. Lanzo. A nonlinear beam finite element for the post-buckling analysis of plate frames by Koiter's perturbation approach. *Computer Methods in Applied Mechanics and Engineering*, 146:325-349, 1997.
- [6] A.D. Lanzo. A Koiter's perturbation strategy for the imperfection sensitivity analysis of thin-walled structures with residual stresses. *Thin-walled Structures*, 37: 77–95, 2000.
- [7] P.N. Poulsen, L. Damkilde. Direct determination of asymptotic structural postbuckling behaviour by the finite element method. *International Journal for Numerical Method in Engineering*, 42:685-702, 1998.
- [8] P.Tiso, M.M. Abdalla, E.L. Jansen. Koiter's Post-buckling analysis of general shell structures using the finite element method. *25th International Congress of the Aeronautical Sciences, Hamburg, Germany*, September 3-8, 2006.
- [9] E. Byskov, J.F. Olesen. Accurate determination of asymptotic postbuckling stresses by the finite element method. *Computer & Structures*, 15:157-163, 1982.
- [10] A.D. Lanzo, G.Garcea, R. Casciaro. Koiter's analysis of thin-walled structures by a finite element approach. *International Journal for Numerical Methods in Engineering*, 38:2325-2345, 1995.
- [11] L. Damkilde, P.N. Poulsen. Direct determination of asymptotic structural postbuckling behaviour by the finite element method. *International Journal for Numerical Methods in Engineering*, 42:685-702,1998.
- [12] B. Budiansky, J.W. Hutchinson. Dynamic buckling of imperfection-sensitive structures. *Proceedings of the 11th International Congress of Applied Mechanics, Munich, Germany*, 1964.
- [13] B. Budiansky. Theory of buckling and post-buckling behavior of elastic structures. *Advances in Applied mechanics*, 14:1-65, 1974.